Quantum Effects on Liquid Dynamics as Evidenced by the Presence of Well-Defined Collective Excitations in Liquid *para*-Hydrogen

F. J. Bermejo,[1] K. Kinugawa,[2] C. Cabrillo,[1] S. M. Bennington,[3] B. Fåk,[4] M. T. Fernández-Díaz,[5] P. Verkerk,[6] J. Dawidowski,[1] and R. Fernández-Perea[7]

[1]*Consejo Superior de Investigaciones Científicas, Serrano 121-123, E-28006 Madrid, Spain*
[2]*Department of Chemistry, Nara Women's University, Nara 630-8506, Japan*
[3]*Rutherford Appleton Laboratory, Chilton, Didcot, Oxon OX11 OQX, United Kingdom*
[4]*Département de Recherche Fondamentale sur la Matière Condensée, SPSMS, CEA, F-38054 Grenoble, France*
[5]*Institut Laue Langevin, BP 156, F-38042 Grenoble Cedex 9, France*
[6]*Interfaculty Reactor Institute, Mekelweg 15, 2629 JB Delft, The Netherlands*
[7]*Argonne National Laboratory, Argonne, Illinois 60439*

(Received 6 December 1999)

The origin of the well-defined collective excitations found in liquid para-H_2 by recent experiments is investigated. The persistence of their relatively long lifetimes down to microscopic scales is well accounted for by calculations carried out by means of path-integral-centroid molecular dynamics. In contrast only overdamped excitations are found in calculations carried within the classical limit. The results provide fully quantitative evidence of quantum effects on the dynamics of a simple liquid.

PACS numbers: 67.20.+k, 62.10.+s, 62.60.+v

In spite of being composed of the simplest stable molecules, the transport and kinetic properties of liquid hydrogen still resist a quantitative understanding [1]. Such peculiar behaviors are usually thought to arise because of the light masses of the particles forming the liquid ($M \approx 2$ amu) and the relatively low temperatures where it exists under its saturated vapor pressure. Quantum effects are thus expected to be noticeable although their relevance for understanding quantitatively most of the transport properties awaits to be established in full. These effects are first manifested by the appearance of a discrete spectrum of transitions between molecular rotational levels. The quantum nature of such motions imposes some symmetry constraints to the total molecular wave function. In particular, the rotational and nuclear spin states of the two protons forming the H_2 molecule are coupled, leading to two distinguishable species, para(p)-H_2 and ortho(o)-H_2 corresponding to molecules having antiparallel ($I = 0$), and parallel ($I = 1$) spin states, respectively. This has an immediate consequence on the symmetry of the interaction potential between H_2 molecules which is isotropic for p-H_2 molecules but angular dependent for o-H_2. It is so because the orientational distribution of the internuclear bond in the laboratory frame is spherically symmetric (s-like) for the former and axially symmetric (p-like) for the latter. A noticeable manifestation of quantum behavior is expected concerning the spatial smearing of the molecular wave function. This comes because of the low molecular mass and the low temperatures in question (about 10–20 K) which makes the thermal (de Broglie) wavelength $\lambda = (2\pi\hbar^2/Mk_BT)$ to reach values larger than the molecular dimensions. In fact, close to triple point, $\lambda \approx 3.3$ Å which becomes comparable to the equilibrium separation between two p-H_2 molecules, $r_0 \approx 3.5$ Å. In addition to the spatial spread of the wave function a delocalization time τ_d can be defined in terms of the fluid number density ρ and the particle mass through [2] $\tau_d = M/2\pi\hbar(\rho/2.612)^{2/3}$, which for the triple point density yields an estimate for $\tau_d \approx 1.2$ ps. Finally, exchange effects arising because of the indistinguishability of the molecules are deemed to play a very minor role since the temperatures in question are well above the quantum degeneracy temperature $T_0 = \hbar/k_B\tau_d = 6.5$ K and therefore most particles will be accommodated in excited levels [3].

Two sets of recent inelastic neutron-scattering experiments [4] have revealed the presence of well-defined (i.e., sharp and long-lived) collective excitations that retain a propagating character up to momentum transfers $Q \approx 0.8$ Å^{-1}. Their wavelengths can be as short as 8 Å and their longitudinal acoustic character was ascertained by analysis of the inelastic structure factors as well as by the approach of their frequencies Ω_Q to the linear hydrodynamic regime $\Omega = c_T Q$ with $c_T = 1096$ m s^{-1} as $Q \to 0$. Their mean-free paths at the lowest explored wave vector were found to be of a few tens of Å's. Finding such well-defined (i.e., phononlike) excitations in an insulating liquid seems difficult to reconcile with what is nowadays known about the dynamics of simple liquids [5] since at scales of a few angstroms and picoseconds one expects finding heavily damped (or overdamped) excitations only, mimicking the well documented case of the heavier rare gases. This comes as a consequence of the highly anharmonic character of the interaction potential $V(r)$. As a rule of thumb [5] only those liquids with an anharmonicity parameter (a sort of effective Grüneisen parameter) $\gamma_G \doteq -r_0/6[V'''(r)/V''(r)|_{r0}] \leq 2$, where the primes are derivatives with respect to r, are believed to be able to support such short wavelength density oscillations. This indeed is the case of molten alkali metals where

excitations of the kind here referred to are sustained because of the long-ranged nature of the metallic binding forces. In contrast, insulating Lennard-Jones (LJ) liquids such as Ar have $\gamma_G \approx 3$ and show no peaks at finite frequencies in their spectra. Liquid He is here the exception to the rule since the sharp excitation spectra is known to emerge as a consequence of the quantum nature of the microscopic dynamics. In the case of hydrogen, the intermolecular potential developed by Silvera and Goldman (SG) [6] is known to provide a reliable representation of the equation-of-state of hydrogen crystals over a wide range of densities [7]. Its shape is somewhat reminiscent of those of LJ form although it shows some significant differences. Because of the symmetry of the problem at hand, only the distance-dependent part of the interactions is relevant, and therefore the molecular interactions will be spherically symmetric. The effective Grüneisen parameter for the SG potential is $\gamma_G = 2.76$, which is closer to that of Ar than to those for molten alkali metals. Therefore, finding long-lived excitations in liquid hydrogen points towards relatively large quantum effects on the liquid dynamics rather than to some peculiarity of the intermolecular potential. Our aim here is thus to unveil the origin of the observed short wavelength excitations, in the hope of shedding some light on the fingerprints of quantum effects on the dynamics of almost-classical liquids. To do this, we compare experimental spectra [4] with those calculated by means of a path-integral-centroid molecular dynamics (PICMD) algorithm [8] as well as with spectra evaluated in the classical limit by conventional molecular dynamics (MD), both using the SG potential to represent the bare interactions.

The PICMD approach [9] uses a path-integral representation for a quasiclassical variable named the centroid which is the average position of the center of the spatial dispersion of the quantum particles. The latter are treated as semiclassical Boltzmann particles and their Newtonian equations of motion are integrated following conventional MD procedures [10]. Within the PICMD formalism, the state of N quantum particles is specified by the partition function given in terms of an analytical continuation to imaginary time of a path-integral representation. This procedure maps the quantum system of N particles to the configurational integral for N classical ring polymers, each one of those representing the path of an individual particle along the imaginary time axis. The centroid is thus defined as the average position of the Feynman path, or equivalently as the position of the center-of-mass of the isomorphic polymer. The dynamics is thus driven by forces generated by an effective potential (the so-called Feynman-Hibbs potential) $V_c(r)$ which can be envisaged as the bare interatomic interaction renormalized by the quantum fluctuation [8,11]. As the same potential is chosen for the classical MD simulations, comparison between both kinds of simulations allows us to gauge the role played by the spreading of the molecular wave function in promoting short wavelength density excitations.

The classical MD employed 613 particles and was run using an NVT code with the density set to 0.0229 Å^{-3} which corresponds to a value close to that of the triple point. Because of their far more complex nature, the PICMD simulations were run for a set of 256 molecules, and details about the procedures followed in the PICMD are given in Ref. [8].

A first assessment of the strength of quantum effects is provided by the comparison of our experimental estimate for the static structure factor $S(Q)$ with those resulting from computer calculations of both PICMD and full classical MD. Figure 1 shows that the maxima of the PICMD are significantly closer to experiment than those of the classical MD. The position of the main peak of the PICMD spectrum centered at about 2.01 Å^{-1} comes rather close to that of the experimental quantity, whereas the $S(Q)$ calculated from classical MD shows significant shifts to larger Q's of all its maxima. This is indicative of a more close-packed liquid structure. In fact, the liquid simulated under the classical regime attains a state of thermodynamic metastability with a density some 8% above the initial value. The system simulated under such conditions lasts as a fluid with a self-diffusion coefficient of 1.6×10^{-5} $\text{cm}^2\,\text{s}^{-1}$ for times at least as long as those explored by the simulations (about 12.5 ns). At densities below 0.030 Å^{-3} the simulated system remains liquid at 14 K and shows a reversible freezing transition into a cubic fcc phase at temperatures between 10–12 K (depending upon the density). In contrast, the PICMD liquid becomes stable with $\rho = 0.0235$ Å^{-3}.

A feature that merits to be noted concerns the sharpness (full width $\Delta Q \approx 0.46$ Å^{-1}) of the first peak of the experimental $S(Q)$ which suggests the presence of significantly

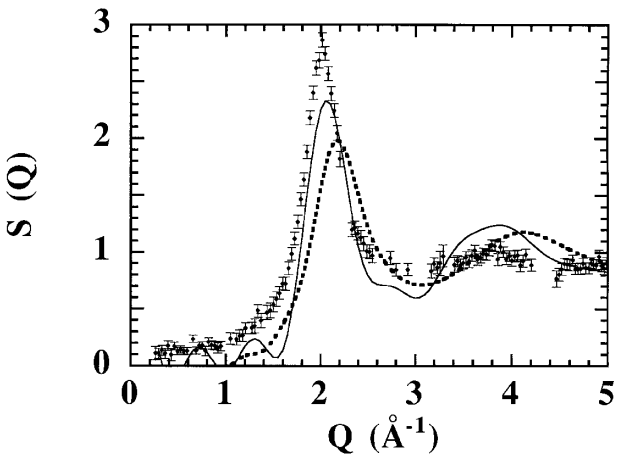

FIG. 1. The symbols with error bars show the experimental estimate for $S(Q)$. The data are described in detail in [4]. The present result incorporates a conventional recoil correction for a particle with $M = 2$ amu, to account for the drop at large Q's of data shown in [4]. The solid line depicts the result from PICMD which are described in more detail in [8], while the dashed line shows the result from classical MD. The high-frequency ripple shown in the PICMD curve arises from truncation errors of the Fourier transform.

longer ranged correlations than those portrayed by the simulations.

A set of spectra of the density correlations [$I(Q,\omega) \propto \langle \rho_Q \rho_Q(\omega) \rangle$] as calculated by PICMD and MD are compared with experiment in Fig. 2. To perform a meaningful comparison we have multiplied the calculated $F(Q,t) = \langle \rho_Q \rho_Q(t) \rangle / N$ intermediate scattering functions by the $R(Q,t)$ instrument response functions so that what are compared are actually the quantities $S_{\mathrm{calc}}(Q,\omega) \otimes R(Q,\omega)$ which are convolutions of the calculated spectra with the experimental frequency windows.

As can be seen from Fig. 2, well-defined excitation peaks (for $\omega \neq 0$) are seen for both experiment and PICMD spectra but are conspicuously absent in spectra simulated under the full classical regime. The first qualitative conclusion is thus that the presence of well-defined collective density fluctuations for wave vectors up to 0.8 $\mathrm{Å}^{-1}$ has to be ascribed to the large quantum effects

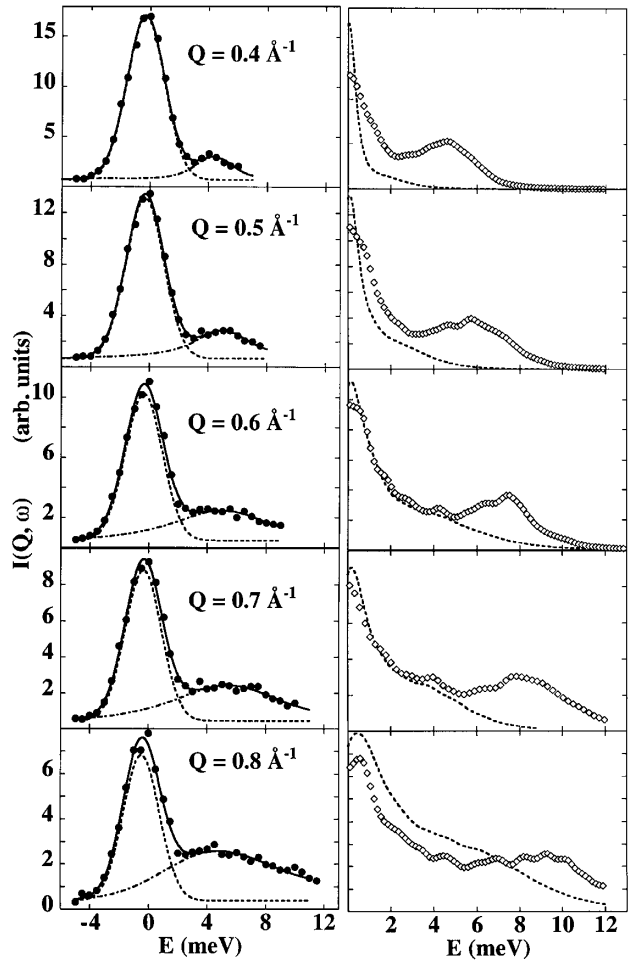

FIG. 2. Experimental $I(Q,\omega)$ spectra (filled symbols) are shown for selected Q values on the left-hand side. Filled symbols represent data actually measured, and the solid line shows the result of the line shape analysis (see text). Dashed and dot-dashed lines show the (quasi)elastic and inelastic components of the experimental spectra. The right-hand side shows simulated spectra. Open symbols are PICMD results and dashed lines those calculated under the classical approximation.

inherent to the regime of low temperatures and light masses. Second, the PICMD spectra show peaks at somewhat higher frequencies than experiment especially at Q values about the maxima of the "dispersion curve." This is understandable on the grounds that the equilibrium liquid density still is somewhat above experiment as referred to above. Finally, while no traces of finite-frequency excitations are found for the classical MD liquid, the frequencies Ω_Q as determined from maxima of $\omega^2 S_{\mathrm{calc}}(Q,\omega)$ approach the hydrodynamic limit in a linear fashion for $Q \leq 0.7$ $\mathrm{Å}^{-1}$.

To put the comparison into more quantitative grounds the spectral line shapes were analyzed in terms of a model for a damped harmonic oscillator $I_{\mathrm{mod}}(Q,\omega) \propto [n_B(\omega) + 1] Z_Q [(\omega^2 - \Omega_Q^2)^2 + 4\omega^2 \Gamma_Q^2]^{-1} \otimes R(Q,\omega)$. The parameters specifying the spectral shape are the amplitude Z_Q, the linewidth Γ_Q, and the peak frequency Ω_Q, where the latter is defined as a renormalized quantity $\Omega_Q^2 = \omega_Q^2 + \Gamma_Q^2$, with ω_Q being the bare (interaction-free) oscillator frequency and, finally, the term with $n_B(\omega)$ stands for the Bose factor.

The wave vector dependence of the parameters giving the excitation frequency and its damping constant (linewidth) is shown in Fig. 3. One sees at a first glance that the parameters of spectra simulated on classical grounds deviate largely from experiment in all the explored Q range. In particular, the damping constant is well above experiment and Ω_Q approaches the low Q regime given by the linear, hydrodynamic dispersion law $\Omega_{\mathrm{hyd}} = c_T Q$ for $Q \leq 0.7$ $\mathrm{Å}^{-1}$. In contrast, both experimental and PICMD frequencies are well above the respective linear laws already for $Q \gtrsim 0.3$ $\mathrm{Å}^{-1}$. The upward departure from a linear hydrodynamic law, usually referred to as anomalous dispersion, is also known from work [12] on liquid ^{3}He, superfluid ^{4}He, and liquid o-D_2, and is at present understood as a mechanism allowing the decay of well-defined excitations [13]. Our data conform to such a view since anomalous dispersion is seen only in the two cases where finite-frequency excitations are clearly seen in the spectra. To quantify such departure, Fig. 3c shows the wave vector dependence of the phase velocities $c_{ph}(Q) = \Omega_Q / Q$. One sees that the shape of $c_{ph}(Q)$ for the PICMD result comes remarkably close to experiment. The most glaring disagreements between PICMD and experiment concern the linewidths above the maximum of the dispersion curve. A plausible reason to explain this concerns the fact that at such short scales the interaction between close enough polymer rings can cause a departure from the spherical symmetry of the bead configuration thus degrading the accuracy of the centroid approximation [11]. Also the fact that the equilibrium liquid density in the PICMD is some 6% above experiment should be taken into account.

Finally, it seems worth delving at some considerations about the explicit mechanisms by which quantum mechanics gives rise to finite-frequency excitations in this anharmonic liquid (as attested by its high γ_G value), while

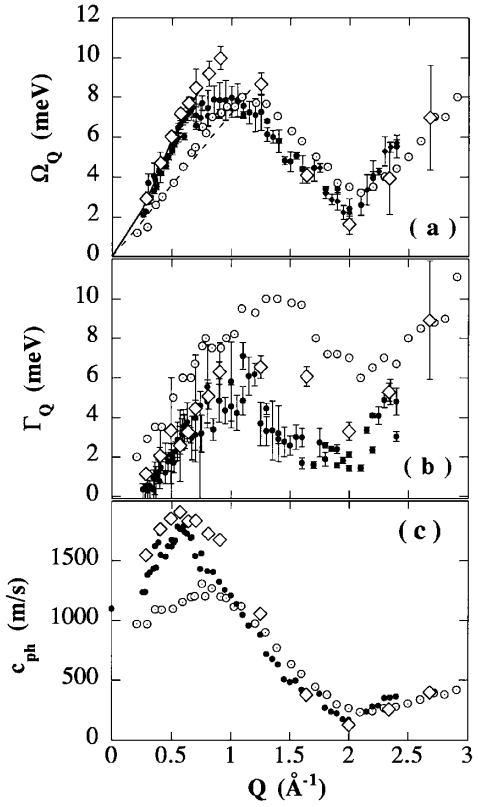

FIG. 3. (a),(b) Wave vector dependence of the spectral parameters. The upper frame depicts the renormalized dispersion frequencies Ω_Q and the middle frame shows the Γ_Q damping constants. Experimental results are shown by filled symbols, open circles with a dot correspond to results from classical MD simulations, and lozenges are PICMD data. The solid line in (a) shows a fit of experimental data to a phenomenological parametrization of the anomalous dispersion (see [4]), and the dashed line depicts hydrodynamic sound. (c) Phase velocities. Same symbols as above are used.

classical dynamics does not. Under the classical regime the anharmonic potential limits the spatial scale of long-lived excitations down to wave vectors not far from the hydrodynamic limit $Q \simeq 10^{-3}$ Å^{-1}. In contrast, our results prove that well-defined excitations are supported by the liquid provided that the bare SG interactions are renormalized by quantum fluctuations. This leads to an effective potential which stabilizes the liquid at substantially lower densities than that of the classical case. Also, the present findings suggest that the main effect of the quantum degrees of freedom is to extend the spatial range of the potential leading to an increase of the characteristic correlation length of the liquid. Microscopically, this causes both real and PICMD liquids to become able to sustain for times of a few picoseconds, liquid configurations where particles collectively oscillate with well-defined frequencies. Such residence times, an estimate of which is given by τ_d are certainly longer than those involved in jumps into another liquid configuration (i.e., hopping out of the "cage") [14]. Taking such values together with the dispersion frequencies one finds that the collective excitations satisfy $\Omega\tau_d \gg 1$ which serves to characterize them as well-defined vibratory motions.

To conclude, the present Letter provides a first experimental confirmation of recent findings on the predictive capability of PICMD to represent the quantum dynamics of highly anharmonic systems [15]. While PICMD should be regarded as exact for harmonic systems, its capability to treat systems driven by highly anharmonic potentials needs to be assessed in lieu of the fact that the errors in the correlation functions resulting from such calculational device grow as the potential becomes more anharmonic [9]. Here we have shown that the harmoniclike behavior revealed in experiment is captured by PICMD. This happens because at the temperatures of interest the centroid dynamics is determined by the ground and first excited state, and this leads to a behavior which manifests itself as quasiharmonic oscillations which show frequencies determined by the curvature of the centroid potential at its minimum. The agreement with experiment is expected to worsen at higher temperatures where several excited states need to be accounted and therefore the anharmonicity of the potential is felt more strongly. This in turn provides a way to characterize the experimental observations as arising from genuine elementary excitations.

[1] J. Rouch *et al.*, Physica (Amsterdam) **88A**, 347 (1977); R. A. Young, Phys. Rev. A **23**, 1498 (1981).
[2] A. F. Andreev, JETP Lett. **28**, 556 (1978); A. F. Andreev and Yu. A. Kosevich, Sov. Phys. JETP **50**, 1218 (1979).
[3] D. M. Ceperley and E. L. Pollock, Phys. Rev. Lett. **56**, 351 (1986).
[4] F. J. Bermejo *et al.*, Phys. Rev. B **60**, 15 154 (1999).
[5] S. W. Lovesey, *Theory of Neutron Scattering from Condensed Matter* (Oxford Science Publications, Oxford, U.K., 1986), p. 214.
[6] I. F. Silvera, Rev. Mod. Phys. **52**, 393–452 (1980).
[7] M. Ross, Rep. Prog. Phys. **48**, 1 (1985).
[8] K. Kinugawa, Chem. Phys. Lett. **292**, 454 (1998); K. Kinugawa, P. B. Moore, and M. L. Klein, J. Chem. Phys. **106**, 1154 (1997).
[9] J. Cao and G. A. Voth, J. Chem. Phys. **101**, 6168 (1994); **101**, 6157 (1994); S. Jang and G. A. Voth, J. Chem. Phys. **111**, 2357 (1999).
[10] G. J. Martyna *et al.*, Mol. Phys. **87**, 1117 (1996).
[11] S. Miura *et al.*, J. Chem. Phys. **110**, 4523 (1999).
[12] For o-D_2 see M. Mukherjee *et al.*, Europhys. Lett. **40**, 153 (1997); see R. Scherm *et al.*, Phys. Rev. Lett. **59**, 217 (1987), for ^{3}He, and H. R. Glyde, *Excitations in Liquid and Solid Helium* (Clarendon Press, Oxford, 1994) Table 10.1, p. 187, for superfluid ^{4}He.
[13] H. J. Maris, Rev. Mod. Phys. **49**, 341 (1977).
[14] The residence times can also be estimated from analysis of the incoherent neutron-scattering law. The values for the self-diffusion coefficient and residence time τ_0 for a mixture of o- and p-H_2 at 15 K are 0.47 Å^2 ps^{-1} and 2.6 ps. P. A. Egelstaff, *An Introduction to the Liquid State* (Oxford Science Publications, Oxford, U.K., 1992), p. 229.
[15] G. Krilov and B. J. Berne, J. Chem. Phys. **111**, 9140 (1999).